Active Sites for Oxygen Evolution Reaction on Pt(111) Electrode

The oxygen evolution reaction (OER) on a Pt(111) surface is significantly enhanced after electrochemical oxidation and reduction cycles. After the third cycle of oxidation/reduction of the Pt(111) surface, the OER activity is nine times higher than that before potential cycles. Surface X-ray diffraction revealed that the active site of the OER after the potential cycles results from the formation of atomic vacancies in the second subsurface Pt layer. The oxidation/reduction potential cycle induces a mortar-shaped roughing of the electrode surface, and the high coordination Pt sites in the atomic size vacancy activates the OER.

Producing hydrogen by using renewable energy and utilizing hydrogen in fuel cells contribute to the attainment of a clean energy cycle. Water electrolysis, which comprises the hydrogen evolution reaction (HER) and the OER occurs at the cathode and anode, respectively, is one of a useful approach to hydrogen production. Although high activity is achieved for the HER in acidic conditions when noble metal electrocatalysts are utilized, the high overpotential of the OER causes large energy loss.

The electrode reactions sensitively depend on the surface atomic arrangement. Recently, the OER activity after holding at various electrode potentials was investigated on single crystal Pt electrodes [1]. Although the atomic arrangement of single crystal electrodes cannot be maintained at positive potentials at which the subsurface oxidation occurs [2], the holding at surface oxidation potentials activates the OER depending on the crystal orientation of substrate. This result indicates that the atomic arrangement of the substrate affects the structure of the Pt oxide. In this study, the surface structure activating the OER induced by electrochemical oxidation/reduction cycles was investigated on the single crystal Pt electrode in 0.1 M $HClO_4$. The electron density profiles including subsurface layer were determined by the measurement of X-ray crystal truncation rod (CTR). The OER activity, which is estimated by the current density at 1.6 V vs reversible hydrogen electrode (RHE), sensitively depends on the atomic vacancies on surface accompanied with surface oxidation/reduction cycle.

During the potential cycling between 0.05 V and 1.6 V vs RHE, the significant OER activation was observed on Pt(111) at the third potential cycles with nine times higher as compared with the activity at the first cycle [3]. After the fourth cycle, the OER activity gradually decreased with continued cycling. This indicates that oxidation/reduction cycles on the Pt (111) surface induce a unique structural change that activates the OER. A characteristic small redox peak appeared at 0.31 V in the hydrogen adsorption/desorption region during the second and the third potential cycles where high OER activity was observed, which was assigned to the atomic vacancies and islands on roughened Pt(111) created by the place exchange of subsurface Pt atoms [4]. The (111) terrace width necessary for vacancy-initiated OER activation was investigated using *n*(111)-(111) series of Pt with the well-defined step and terrace structure, where *n* is the number of terrace atomic rows. Enhancement of the OER activity by successive potential cycling was observed on the surfaces where the terrace width is greater than five atomic rows ($n > 5$). This result suggests that the formation of vacancies with sizes larger than 3 missing atoms, such as $V_{3\text{-}0}$ shown in **Fig. 1(a)** can trigger OER activation. The OER active sites appear to arise from the oxidation of Pt atoms located inside atomic vacancies larger than $V_{3\text{-}0}$.

The electron density along the surface normal direction containing the subsurface was determined using specular and non-specular X-ray CTRs (**Fig. 1(b)**). The potential-cycle dependence of the depth profile of the atomic density for an atomic size vacancy was evaluated from the average occupancies of the Pt layers. X-ray measurements were taken at 1.0 V following a scan to 1.6 V to prevent further oxidation caused by holding the potential at 1.6 V. Further oxidation or reduction of Pt oxide does not occur at 1.0 V. Before the potential cycles (0 cycle), the oxygen layer is located at 2.3 Å from the Pt2 layer, which is assigned to the oxygen atoms of the adsorbed water or hydroxide species. The occupancy of the first Pt oxide layer (Pt_3) is less than 0.2 at the first cycle, indicating a rough surface with irregularities caused by the formation of vacancies and islands, as shown in **Fig. 1(c)**. After the second cycles, which activates the OER, is accompanied by a reduction in the occupancy of the PtO layers (Pt_3 and Pt_2), and a decrease in the occupancy of the subsurface Pt_1 layer from 0.99 to 0.91. These observations suggests that the defect sites are produced at the subsurface Pt_1 layer of the vacancies. Vacancies larger and deeper than $V_{3\text{-}0}$, such as $V_{3\text{-}1}$ and $V_{7\text{-}3}$, are required to form defects at the subsurface Pt_1 layer, as shown in **Fig. 1(a)**. X-ray structural analysis indicates that the layer spacing between Pt_1 and Pt_2 in the subsurface is comparable to that of bulk Pt. Therefore, the bottom of the vacancy (the Pt_1 layer) maintains its metallic state. The bottom Pt atom retains a large coordination number, which results in a lower binding energy for adsorbed oxygen.

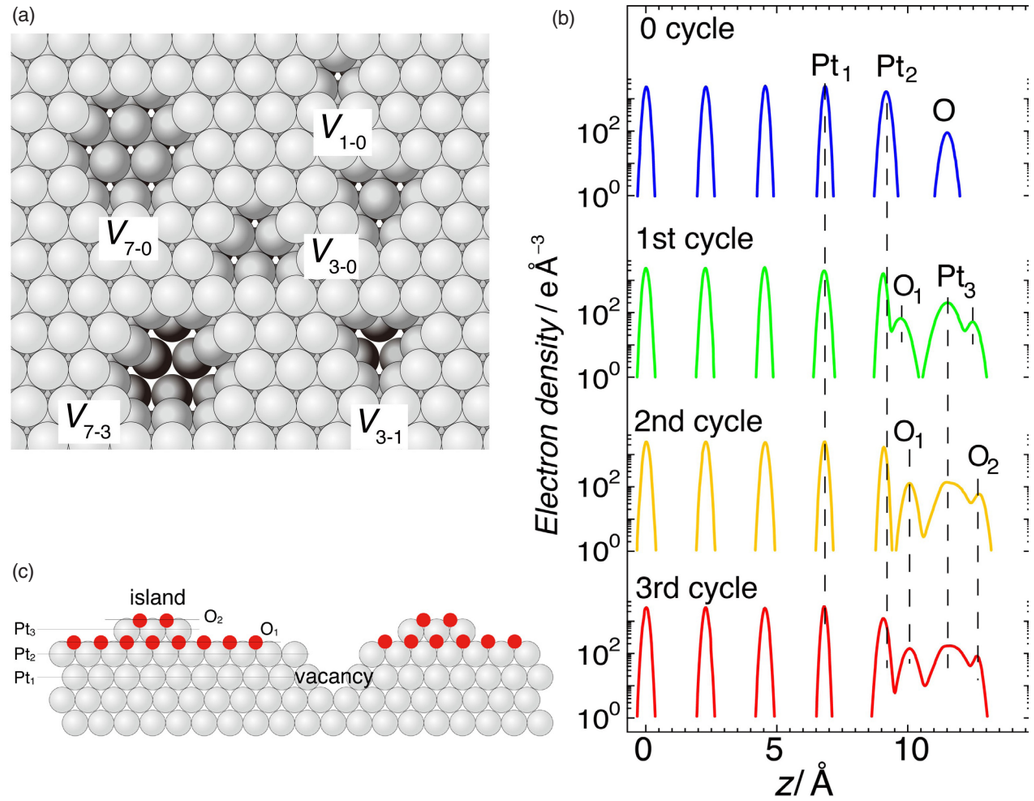

Figure 1: (a) Hard-sphere model of atomic size vacancies, $V_{x\text{-}y}$, formed on the (111) facet, where *x* and *y* denote the number of extracted atoms in the topmost surface and the second subsurface layers, respectively. **(b)** Electron density profiles along the surface are normally optimized using specular and non-specular CTRs for each cycle. **(c)** Schematic diagram of the side view of the PtO layer on Pt(111). Pt and oxygen atoms are represented by gray and red spheres, respectively.

REFERENCES

[1] F. Bizzotto, H. Ouhbi, Y. Fu, G. Wiberg, U. Aschauer and M. Arenz, *ChemPhysChem* **20**, 3154 (2019).
[2] M. Ruge, J. Drnec, B. Rahn, F. Reikowski, D. A. Harrington, F. Carala, R. Felici, J. Stettner and O. M. Magnussen, *J. Am. Chem. Soc.* **139**, 4532 (2017).
[3] K. Iizuka, T. Kumeda, K. Suzuki, H. Tajiri, O. Sakata, N. Hoshi and M. Nakamura, *Commun. Chem.* **5**, 126 (2022).
[4] L. Jacobse, M. J. Rost and M. T. M. Koper, *ACS Cent. Sci.* **5**, 1920 (2019).

BEAMLINE

BL-3A

K. Iizuka,[1] T. Kumeda,[1] H. Tajiri,[2] O. Sakata,[2] N. Hoshi[1] and M. Nakamura[1] ([1]Chiba Univ., [2]JASRI)